J Fluoresc (2015) 25:283–295
DOI 10.1007/s10895-015-1507-3

ORIGINAL PAPER

The Effect of Ring Size on the Optical Behavior of Novel Photochromic Push-Pull Dyes

Safaa El-din H. Etaiw · Tarek A. Fayed · Marwa N. El-Nahass · Rehab S. Youssif

Received: 12 October 2014 / Accepted: 2 January 2015 / Published online: 24 February 2015

Abstract The photophysical behaviors of newly synthesized photochromic dyes have been investigated in different solvents of various polarities using steady-state absorption and emission techniques. It was found that, the absorption and emission spectra of these dyes depend on the ring size and the solvent polarity. The higher values of the dipole moments of the investigated dyes in the excited state than those in the ground state suggest that these dyes can serve as good candidate components of nonlinear optical materials. Additionally, the photoisomerization parameters (percentage of composition of cis isomers and quantum yields of photoisomerization) depend on the polarity and the viscosity of the used solvents as well as the ring size. The molecular motion that occurs in the isomerization process has facilitated the development of molecular devices. Finally, the halochromic behaviors of the investigated dyes promise them to act as acid–base indicators.

Keywords Photochromic dyes · Ring size · Photoisomerization · Molecular devices · Halochromic behaviors

Electronic supplementary material The online version of this article (doi:10.1007/s10895-015-1507-3) contains supplementary material, which is available to authorized users.

S. E.-d. H. Etaiw · T. A. Fayed · M. N. El-Nahass (✉) · R. S. Youssif
Chemistry Department, Faculty of Science, Tanta University, Tanta 31527, Egypt
e-mail: marwacu@yahoo.com

M. N. El-Nahass
e-mail: marwa.elnahas@science.tanta.edu.eg

Introduction

Push-pull dyes with donor-acceptor moieties are not only having importance in photophysical, photochemical and photobiological processes [1, 2], but also having potential applications in the technological developments. Among various types of push-pull ones, diarylethylenes, DAEs which are widely used as sensitizers and other additives in the photographic industry [3]. In diarylethylenes, the donor and acceptor groups are joined by suitable conjugation, involving either single or multiple enyl groups. They show strong intramolecular charge transfer (ICT) character in their electronic states, especially in their excited electronic states [4, 5]. Accordingly, these dyes show very strong solvent polarity dependent changes in their photophysical characteristics, namely, a large red shift in the emission spectra with increasing solvent polarity, exceedingly high solvent polarity dependent changes in the Stokes' shifts between absorption and fluorescence spectra, significant reduction in the fluorescence quantum yields (ϕ_f) and lifetimes (τ_f) on increasing the solvent polarity, etc. [6]. Though literature on the photophysical behavior of DAEs is quite large [7–9], there are many aspects of their excited states that remain to be understood clearly. The donor-acceptor kind of DAEs can undergo the two important photoinduced processes in their excited states and they are, (i) the cis-trans isomerization which takes place via the rotation of the molecule around the double bonds, and (ii) the formation of the TICT state which takes place via the rotation of the molecule around a suitable single bond in combination with the complete transfer of an electron from donor moiety to the acceptor moiety [10]. Either of these processes introduces an additional nonradiative deexcitation channel for the excited dyes, in addition to their usual internal conversion (IC) and intersystem crossing (ISC) processes [11–13]. Moreover, depending on the polarity of the solvent medium, the propensity of these nonradiative processes introduced by the participation in the isomerization/TICT

process can sometimes be so strong that they lead to unusually large reduction in the ϕ_f and τ_f values of the dyes [14–16]. As the literature reports indicate, the isomerization mediated nonradiative process for DAEs is mainly dominated at the lower solvent polarity region while the nonradiative process related to the TICT formation is mainly dominated at the higher polarity regions of the solvents [17]. These characteristic structural features make them to display very high first-order hyperpolarizability which in effect makes these dyes as the efficient materials for molecular electronics applications [18, 19], for nonlinear process like second harmonic generation [20–23] and also as optical materials [24–26]. DAEs are also known to have many applications in biological sciences as fluorescence probes [27–29], in polymer sciences as free-radical photoinitiators [30] and in dye sensitized solar cells as efficient photoelectric conversion dyes [31, 32].

Benzoxazole moeities find extensive use in the industrial purposes and the interest in their chemistry has increased due to the application of such moieties in photosensitization or in valuable optical brighteners [33] and in analytics [34]. Dye organization is also considered to be the key to advanced functional organic materials for electronics and photonics [35, 36]. Some of these dyes are growth inhibitors to bacteria [37] and to the mitosis of fertilized sea urchin eggs [38]. They possess hormonal effects on plant growth [39] and can be used for the determination of the sensitivity of micro-organism to antibiotics [40]. They can also be used as laser dyes [41, 42] and producing offset printing plates [43].

Photochromism is the reversible light-induced transformation of a compound between two forms having different absorption spectra [44]. During photisomerization not only optical properties such as the absorption spectra but also molecular properties such as refractive indices, ionization potentials and dielectic constants, dipole moments and electronic characteristics are changed reversibly. Photochromic materials have been garnering interest for over a decade because so far they are the most favorable candidate for ultrahigh density optical memory media or optical switching device materials DAEs with heterocyclic aryl groups are remarkable photochromic systems where the chemical transformation is single bond breaking. Because the distribution of π-bonds is different in both isomers, they have distinct absorption spectra. They are well known to have different characteristics such as good thermal stability for both isomers, high fatigue resistance in isomerization, and rapid response [45]. These photochromic systems might have potential use in applications such as optical data storage units, trigger elements, or as switching devices in optical data processing.

In the present work, the photophysical and photochemical behaviors of newly synthesized diarylethylenes namely:- 1-(phenyl)-2-(2-benzoxazolyl)ethylene, StBOX, 1-(1-naphthyl)-2-(2-benzoxazolyl)ethylene, NBOX, 1-(9-phenanthryl)-2-(2-benzoxazolyl)ethylene, PBOX and 1-(9-pyrenyl)-2-(2-benzoxazolyl)ethylene, PyBOX has been studied. We thus gained a better understanding on the effects of the molecular structure and the solvent which may help to design suitable diarylethylene molecules possessing appropriate photochemical reactivity and laser properties. The correlation between the experimental results and the theoretical ones using semiemperical quantum calculations has been discussed. Finally, the acid–base equilibrium reactions of diarylethylenes in aqueous medium have been studied.

Experimental

The investigated photochromic diarylethylenes namely:- 1-(phenyl)-2-(2-benzoxazolyl)ethylene, StBOX, 1-(1-naphthyl)-2-(2-benzoxazolyl)ethylene, NBOX, 1-(9-phenanthryl)-2-(2-benzoxazolyl)ethylene, PBOX and 1-(9-pyrenyl)-2-(2-benzoxazolyl)ethylene, PyBOX were synthesized by condensation of 2-methylbenzoxazole with the corresponding arylaldehyde (benzaldehyde, α-naphthaldehyde, 9-phenanthraldehyde and 9-pyrene carbaldehyde) as reported previously [46]. The synthetic route of these compounds with their abbreviations was shown in Scheme S1 in the supplementary materials. The investigated diarylethylenes were synthesized as follow: Equimolar quantities of 2-methylbenzoxazole and the corresponding aldehyde (benzaldehyde,α-Napthaldehyde, 9-phenathraldehyde and 9-pyrene carbaldehyde) were dissolved in an alkaline dimethylformamide solution (containing 5 gm KOH / 100 ml) then the solution was stirred for about 3 h, after that drops of 0.2 N HCl were added to the pre-cold reaction mixture till complete precipitation. The products were separated out by filtration and purified by recrystalization twice from dry ethanol. The reactions yielded crystals having yellow color. Finally, the purity of the prepared compounds was confirmed by FT-IR and mass spectral measurements. The mass spectra of the investigated compounds, StBOX, NBOX, PBOX and PyBOX give the molecular ion peaks at the desired positions: m/z=220, 270, 319 and 348, respectively. The obtained molecular ion peaks showed that m/z is equivalent to molecular weight of the proposed compounds. Hence m/z value confirms the molecular weight of compounds, (Fig. S1, in the Supplementary materials). The IR spectra showed sharp bands at vibrational frequencies within the range (1454–1633 cm^{-1}) and (1574 cm^{-1}) characteristic for the ethylenic C=C double bond. In addition, the spectra showed bands within the range 956 to 1069 cm^{-1} due to out of plane bending vibration of CH=CH. Also, weak bands are observed in the range 2815–2919 cm^{-1} and can be ascribed to the stretching vibrations of the aliphatic C-H bond, (Fig. S2, in the Supplementary materials).

Spectroscopic grade solvents (from Aldrich or BDH) were used as received. All solvents were non-fluorescent in the region of fluorescence measurements.

Double distilled water was used for the preparation of buffer solutions. Analytical grade orthophosphoric acid and NaOH were used as received.

Aqueous buffer solutions were prepared by mixing appropriate volumes of NaOH and H_3PO_4, 0.1 M each. Solutions having pH<2 were prepared following Hammett's acidity (H_o) scale [47, 48].

Steady state electronic absorption was recorded on a Shimadzu UV-3101 PC spectrophotometer, while the steady-state fluorescence spectra were recorded using a Perkin-Elmer LS 50B scanning spectrofluorometer, using matched quartz cuvettes.

Continuous irradiation of solutions during trans-cis photoisomerization measurements were carried out in the same cell of the fluorometer which is equipped with a 10 kW Xe-Lamp and a monochromator where both the intensity and wavelength of the excitation light could be controlled easily. The solution was shacked periodically and its absorption spectrum was recorded after known time intervals.

The fluorescence quantum yields (ϕ_f) were measured relative to 9,10-Diphenylanthracene in EtOH as a standard (ϕ_f= 0.95) [47, 48]. The samples were excited around their absorption maximum. For determination of the trans→cis photoisomerization quantum yields (φ_t), the method described by Gauglitz [49] was used. All measurements were carried out under red light at 25 °C±1 using fresh solutions (2×10^{-5} M).

Geometry optimization along with electronic structures and dipole moment calculations of both the ground and excited state of the investigated ketocyanines have been performed using Portable HyperChem 8.0.7 with the help of ArgusLab 4.0 software (Mark A. Thompson, Planaria Software LLC, Seattle, WA) [50]. Precise geometry optimization was obtained by PM3 Hamiltonian, while electronic structure and dipole moments were calculated by PM3 and ZINDO/S methods. All calculations were performed using the default parameters.

Results and Discussion

Theoretical Calculation

In order to give clear picture on the ground and excited state properties of the investigated diarylethylenes, depending on the effect of ring size, the theoretical calculations have been done using PM3 semiempirical calculations. Figure 1, shows the geometrical and electronic structures of all concerned dyes, StBOX, NBOX, PBOX and PyBOX in the ground state. The full optimized geometry of StBOX shows stable planar structure with a minimum energy when all the dihedral angle equals to 0° or 180°. However, the semiemperical calculations showed some deviation from planarity for NBOX and PBOX

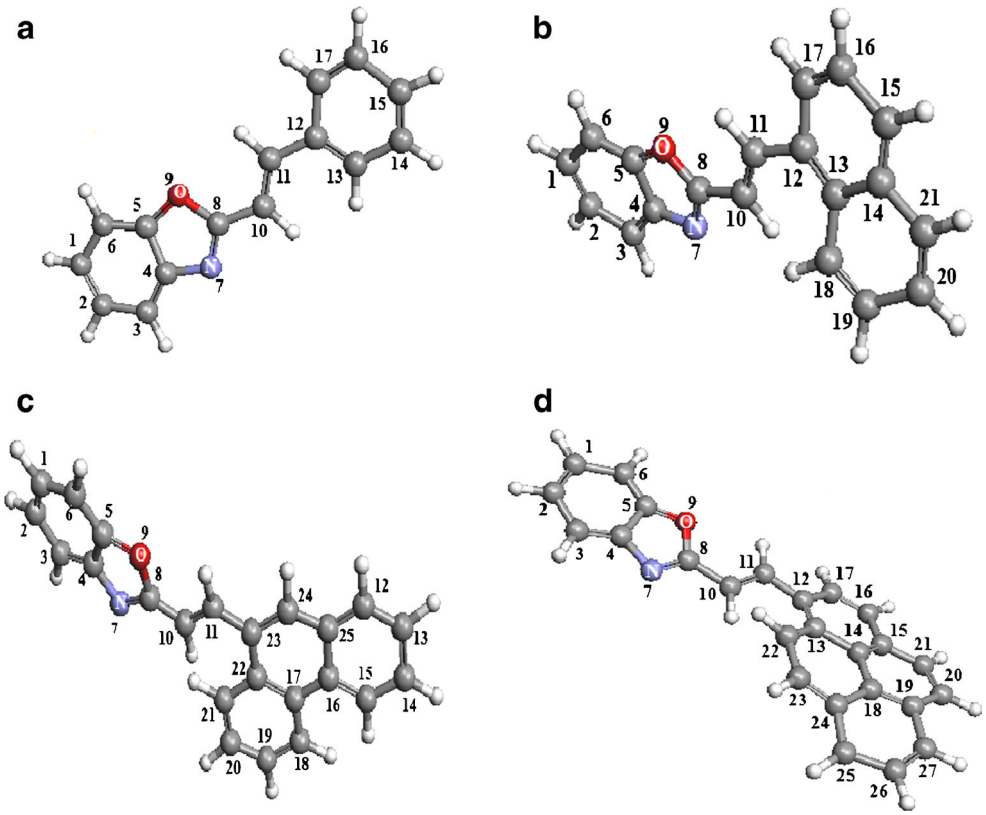

Fig. 1 Optimized geometry of ground state **a** StBOX, **b** NBOX, **c** PBOX and **d** PyBOX using PM3 calculations

due to the small twisting of the naphthyl and phenanthryl rings, respectively along with the ethylenic bridge. In case of NBOX, the torsion angle for C11, C12, C13 and C18 is 43.43°. While, in case of PBOX, the torsion angle for (C10, C11, C23 and C22) is 16.59°. Also, PyBOX has stable twisted structure with torsion angle for C10, C11, C12 and C13 equals to 153.2°. Additionally, in order to explore the direction of the intramolecular charge transfer, the charge distribution on the different units over the whole molecular skeleton in the ground and excited states as well as the orbital topologies of HOMOs and LUMOs levels of the investigated compound have been elucidated and shown in Fig. 2. As can be seen, the charge density on the benzoxazole moiety increases upon excitation, and is accomplished by decreasing of the charge density at the aryl moiety. The HOMO–LUMO representation indicates that there is a charge transfer from aryl and benzoxazole moeities, which could be considered as a donor center, to benzoxazole moiety as an acceptor one. Within these dyes, there is a gradual increase of charge separation upon excitation, on going from phenyl to pyrenyl derivatives. This reflects the increasing of the efficiency of ICT with increasing the ring size.

Solvatochromic Behavior of the Investigated Diarylethylenes

In order to have a better understanding about the effects of molecular structure and ring size on the spectral behavior of the investigated diarylethylenes, the absorption and emission spectra have been studied in different solvents of various polarities and hydrogen bonding abilities including Gly, EtOH, $CHCl_3$, ACN and Hex and the data were collected in Table 1. Figure 3 shows the normalized absorption spectra of the investigated dyes in $CHCl_3$. As can be seen, the absorption band of NBOX, PBOX and PyBOX undergoes red shifts with increasing the ring size (ca. 28, 26 and 45 nm, respectively relative to that one for StBOX). This absorption band could be attributed to the intramolecular charge transfer (ICT) between the benzoxazolyl and aryl fragments via the ethylenic bridge. On the other hand, the absorption spectra of PyBOX distinct vibrational structure in both polar and non polar solvents, however those of NBOX and PBOX are broad structurless band. This may be attributed to localization of the transition due to the weak interaction between both the molecular parts of PBOX which confirmed by its stable twisting structure compared to the small twisting of the naphthyl

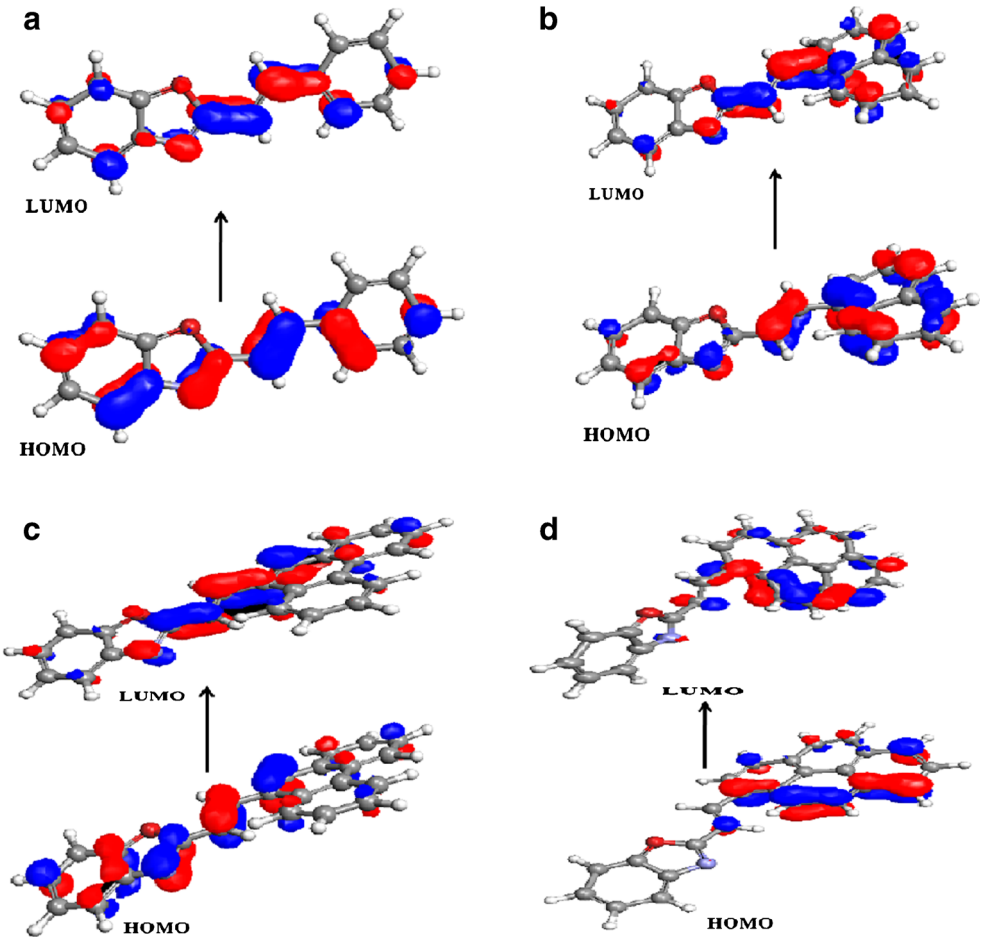

Fig. 2 HOMO—LUMO representation of **a** StBOX, **b** NBOX, **c** PBOX and **d** PyBOX using PM3 calculations

Table 1 Spectroscopic data of the investigated diarylethylenes in different solvents of various polarities at 298 K

Dye	Solvent	λ_a^{max} (nm)	ε_{max} (M^{-1} cm^{-1})	λ_f (nm)	ϕ_f
StBOX	Hex	320	33,850	378^{max}	0.067
	$CHCl_3$	324	44,000	390^{max}	0.04
	ACN	321	34,900	384^{max}	0.046
	EtOH	323	33,760	404^{max}	0.034
	Gly	328	33,490	392^{max},410	0.083
NBOX	Hex	345	36,390	$393,414^{max}$,438^{sh}	0.071
	$CHCl_3$	351	31,000	430	0.022
	ACN	348	34,960	427	0.019
	EtOH	350	34,320	429	0.014
	Gly	359	31,420	430	0.098
PBOX	Hex	343	34,580	$400,423^{max}$,446^{sh}	0.12
	$CHCl_3$	350	38,100	437	0.043
	ACN	345	33,790	430	0.02
	EtOH	351	34,030	435	0.013
	Gly	357	34,730	446	0.178
PyBOX	Hex	387	49,770	$434,460^{max}$, 488^{sh}	0.704
	$CHCl_3$	395	51,700	464	0.085
	ACN	384	55,710	470	0.09
	EtOH	386	46,050	473	0.102
	Gly	400	33,140	487	0.49

^{max} refers to the intensity of the highest peak

^{sh} refers to the shoulder peak

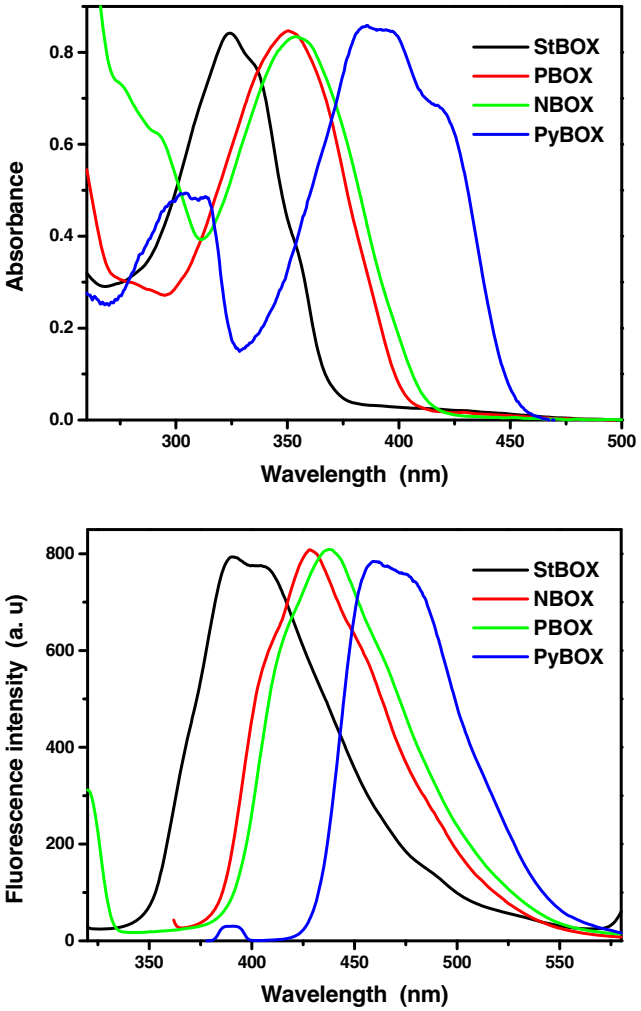

Fig. 3 Normalized absorption and emission spectra of the investigated diarylethylenes in $CHCl_3$

and phenanthryl rings, respectively. Similarly, the fluorescence spectra of the investigated dyes are found to be mirror images to the corresponding long wavelength absorption band. There is a significant bathochromic shift in the emission maxima on going from StBOX to PyBOX. The ring size-based red shift in both absorption and emission maxima can be attributed to lengthening of the conjugated system. Replacement of phenyl ring with a larger polycyclic group, naphthyl, phenanthryl and pyrenyl moieties enhances the resonance delocalization of the π-electrons and leads to progressive shifts in the spectral maxima.

Additionally, from the data reported in Table 1, it is evident that the fluorescence spectra of NBOX and PBOX and PyBOX appear as structurless bands in polar solvents, while, in non-polar solvents the emission bands are structured. It was found that the emission spectrum of NBOX, PBOX and PyBOX in Hex fluoresces with vibronic structure at (393, 414 nm, (400,423 nm) and (434, 460 nm), respectively, in addition to a shoulder at 438, 446 and 488 nm, respectively. This is attributed to the vibrational coupling of the vinyl hydrogens. Also, the obtained data indicate that the excited singlet state of these dyes is more polar than their ground state, which led to this high sensitivity to the solvent polarity. The high solvatochromaticity and broad featureless of the emission spectra indicate intramolecular charge transfer nature of the excited state. The obtained results confirmed that as the size of the aryl ring increases, its electron-donating ability increases and the aryl ring transfers some of its charge to the benzoxazole moiety, leading to increase the extent of ICT between the benzothiazolyl and aryl fragments which confirmed by the red shift of their various spectra.

The solvatochromic shifts of the emission of the dyes under investigation cannot be explained only by the basis of mode of the solute-solvent interaction. Therefore, the fluoresence spectra are correlated with a combination of several solvent parameters (nonspecific solvation, electrophilic solvation, and others). There are many correlation equations based on the use of several independent parameters, in order to describe the solvatochromic shifts [51]. Among these methods one called solvatochromic comparison method (SCM) has been proposed by Kamlet et al. [52]. This approach separates the dielectric effects of solvents (π*), hydrogen-bond donor (α) and acceptor (β) abilities of the solvents on the spectral

properties. So, the obtained fluorescence energy has been analyzed using the SCM according to the following correlations:

for StBOX	$E_{(A)}$=88.42–0.93 α +2.18 β – 0.67 π*
	$E_{(F)}$=73.5–4.92 α +7.6 β – 1.72 π*
for NBOX	$E_{(A)}$=81.5–0.01 α+1.1 β - 1.02 π*
	$E_{(F)}$=70.6–0.92 α +5.69 β – 1.51 π*
for PBOX	$E_{(A)}$ =81.8–0.28 α +0.29 β – 0.57 π*
	$E_{(F)}$=70.6–0.9 α+5.67 β – 1.5 π*
for pyBOX	$E_{(A)}$=63.49–2.01 α +0.97 β – 1.93 π*
	$E_{(F)}$=68.06–4.38α+4.09β - 2.67 π*

The negative value of coefficient of π* is a sign of stabilization due to dipolar interactions which attributes to the observed bathochromic shift in absorption band with increasing polarity of the solvents. In addition, the higher magnitudes of the coefficients of α and β in the excited state indicate that dipole-dipole interactions, hydrogen-bond donor (α) and acceptor (β) abilities of the investigated dyes contribute more to the stabilization of excited state than that of ground state. The higher coefficients of them at the excited state than that in ground state is attributed to the greater extent of dipole-dipole interaction at the former state and confirms that the excited state dipole moment of the investigated dyes is much higher than the ground state dipole moment. Moreover, higher magnitude of the coefficient of α in the excited state than that in the ground state supports the fact that there is a greater extent of the extent of ICT between the benzothiazolyl and aryl fragments.

Also, in order to assess the sensitivity of the investigated dyes to the polarity of the solvents and the ring size, the difference between dipole moment in the ground (μ_g) and excited (μ_e) states has been determined via implementation of Bakhshiev's [53] and Kawski-Chamma-Viallet's equations [54].

$$\Delta\overline{\nu}_{st} = \nu_{abs} - \nu_{em} = \frac{2\left(\mu_e - \mu_g\right)^2}{hca^3} f(\varepsilon, n) + constant(\text{Bakhshiev's equation})$$

$$\nu_{abs} + \nu_{em} = -\frac{2\left(\mu_e^2 - \mu_g^2\right)}{hca^3}[f(\varepsilon, n) + 2g(n)] + constant(\text{Kawski–Chamma–viallet's})$$

Where, $f(\varepsilon, n) = \frac{2n^2+1}{n^2+2}\left[\frac{\varepsilon-1}{\varepsilon+2} - \frac{n^2-1}{n^2+2}\right]$ g(n) $= \frac{3}{2}\left[\frac{n^4-1}{(n^2+2)^2}\right]$ Where ν_{abs} and ν_{em} are the absorption and fluorescence band shift in solvents of varying permittivity (ε), refractive index (n), f(ε,n) is the solvent polarity parameter, "a" is the Onsager cavity radius, h is the Plank's constant and c is the speed of light. The cavity radius was taken as 40 % from the distance between the two farthest atoms in the direction of charge separation within the molecule [55], which was estimated following geometry optimization of StBOX, NBOX, PBOX and PyBOX using PM3 semiempirical calculations with the help of ArgusLab 4.0 software (Mark A. Thompson, Planaria Software LLC, Seattle, WA) [50]. The cavity radius comes out to be 5.4, 5.44, 5.9 and 6.26 A°, respectively. The dipole moments of the investigated diarylethylenes in the ground and excited states have been determined from the slopes m_1 and m_2 and were summarized in Table 2. As reported, the excited-state dipole moment is larger than that of the ground state. The increase in dipole moment explains the red shift in the absorption spectra with increasing the solvent polarity. This is attributed to ICT and confirms the competition between the two main subunits of molecules (benzoxazolyl and aryl moeities). The large difference between the dipole moments of StBOX, NBOX, PBOX and PyBOX at ground and excited states is consistent with the higher extent of contribution of dipole-dipole interaction towards the stability of excited state than that of ground state which confirms the above explanation. The excited-state dipole moment is larger than that of the ground state. The increase in dipole moment explains the significant bathochromic shift in the absorption spectra with increasing the solvent polarity. This is attributed to competition between the two main subunits of molecules, the benzoxazole moiety and the aryl ring via the ethylenic bridge. The effect of the ring size on the dipole moment of the concerned dyes in the ground and excited states is very significant. The dipole moment increases with the ring size in the order StBOX<NBOX<PBOX<PyBOX which reflects the role of the electron-donating nature in increasing the ICT interaction, and thus greater solvent relaxation. This result suggests that these dyes can serve as good candidate components of nonlinear optical materials. The obtained values are in a good agreement with those calculated theoretically using semiempirical quantum calculations, Table 2.

Also, the fluorescence quantum yields (Φ_f) of the investigated diarylethylenes have been measured in the selected solvents, and summarized in Table 1. The data show that

Table 2 Ground and excited states dipole moments (μ_g, μ_e), and slopes (m_1, m_2) of the investigated diarylethylenes

Dye	Experimental				Theoretical	
	μ_g (D)	μ_e (D)	m_1 (cm^{-1})	m_2 (cm^{-1})	μ_g (D)	μ_e (D)
StBOX	0.28	4.36	1155	2130	0.321	2.34
NBOX	0.83	4.95	1006.3	2036	0.54	4.53
PBOX	1.33	5.53	850	4071	2.85	5.9
PyBOX	2.8	7.2	4164	5506	3.9	7.9

the Φ_f is highly sensitive to the size of polycyclic group, the nature and the refractive index of the solvent. The Φ_f values decrease steadily as the hydrogen bond donating ability of the solvents increases indicating that hydrogen bonding interactions are controlling strongly the decay of excited dye molecules. For example, the ϕ_f values of StBOX, NBOX, PBOX and PyBOX decrease by 1.9, 5.0, 7.1 and 7.0 folds on going from Hex to EtOH, respectively. This is due to the coupling between the close lying n–π* and π–π* states which increases the possibility of non-radiative transitions to deactivate the excited state [56]. As can be seen, PyBOX has high ϕ_f values in all the mentioned solvents compared to those for the other dyes. This means that PyBOX is highly fluorescent dye, indicating the non-radiative transitions from the excited state and confirms the ring size dependence of the quantum yield.

Photochromic Behavior of the Investigated Diarylethylenes

The photochemical trans-cis isomerization of the investigated dyes was studied at room temperature in different solvents having various polarities like EtOH, ACN, c-hexane and Gly as an example for viscous solvent, Fig. 4. The quantities of the cis isomers at the photostationary states (%cis), the quantum yields of the photoisomerization processes ($\phi_{t\rightarrow c}$ and $\phi_{c\rightarrow t}$), the photoequlibrium constant (K_{ph}^{pss}) and the partial rate constants for the forward $k_{t\rightarrow c}$ and the backward $k_{c\rightarrow t}$ reactions, at two different irradiation wavelengths, have been determined and summarized in Table 3. The obtained results have been related to the ring size, the solvent characteristics (polarity and viscosity) and the excitation wavelength.

The determination of trans-cis photoisomerization quantum yields and the corresponding photoreaction parameters of the investigated dyes, in Hex at λ_{irr}=365 nm, would be

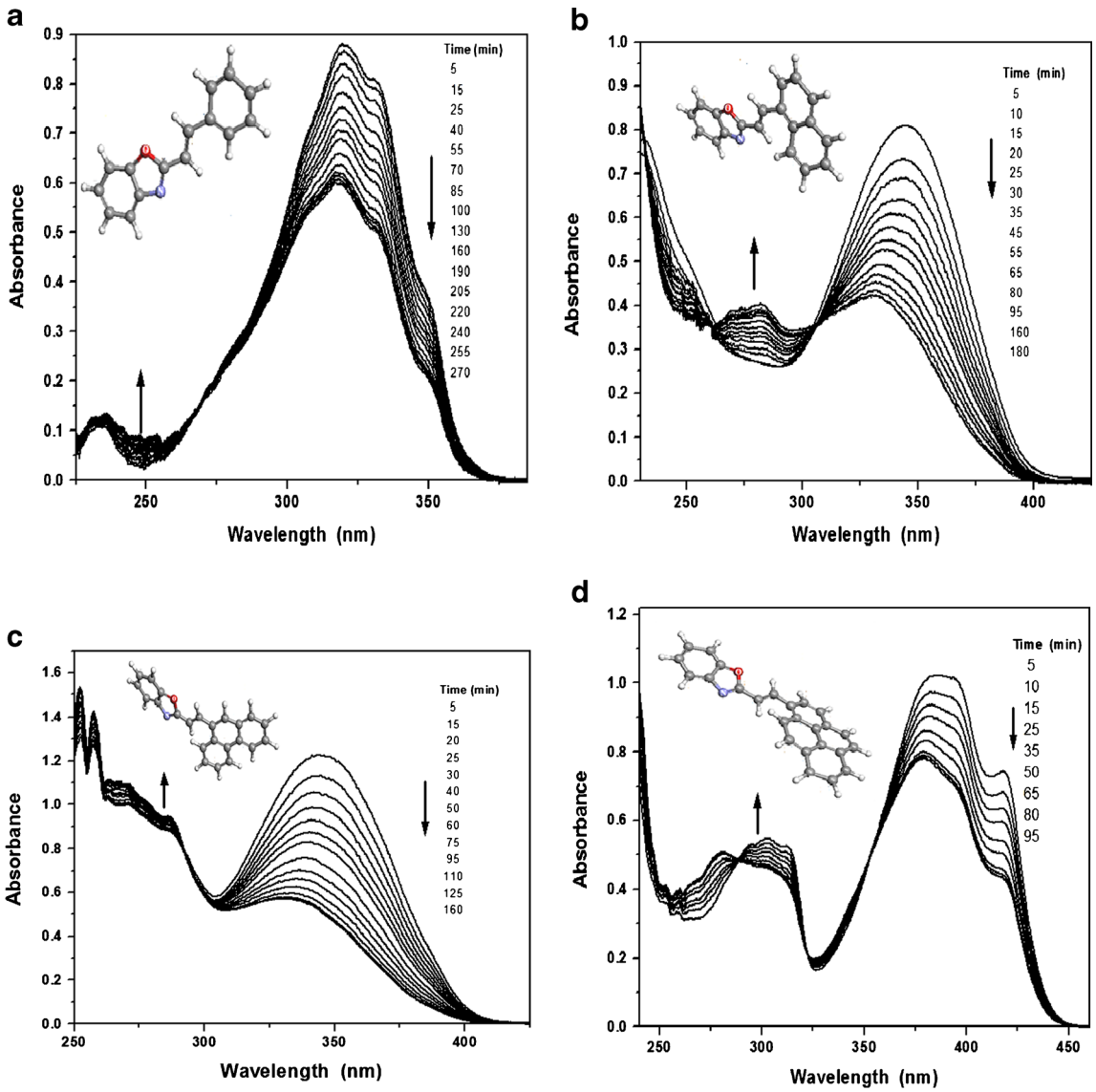

Fig. 4 Absorption spectra of **a** StBOX **b** NBOX **c** PBOX, and **d** PyBOX in Hex at 365 nm. The irradiation times are indicated in the Figure

Table 3 Photochemical data for the trans-cis photoisomerization of the investigated diarylethylenes in different solvents at different irradiation wavelengths at room temperature

	% cis	$\Phi_{t\rightarrow c}$	$\Phi_{c\rightarrow t}$	$K_{t\rightarrow c}$ (10^{-4} s^{-1})	$K_{c\rightarrow t}$ (10^{-4} s^{-1})	% cis	$\Phi_{t\rightarrow c}$	$\Phi_{c\rightarrow t}$	$K_{t\rightarrow c}$ (10^{-4} s^{-1})	$K_{c\rightarrow t}$ (10^{-4} s^{-1})
StBOX	λ_{irr}=313 nm					λ_{irr}=365 nm				
EtOH	76	0.053	0.038	5.9	1.4	70	0.06	0.044	6.5	1.23
ACN	82	0.059	0.034	6.1	1.3	85	0.07	0.043	7.4	1.22
Hex	82	0.041	0.032	4.1	1.5	78	0.05	0.04	5.6	1.4
Gly	54	0.03	0.033	2.9	1.2	58	0.044	0.046	3.1	1.2
NBOX	λ_{irr}=365 nm					λ_{irr}=405 nm				
EtOH	71	0.236	0.051	4.3	1.151	76	0.055	0.144	5.7	4.3
ACN	80	0.75	0.048	5.4	2.32	84	0.06	0.135	6.12	5.14
Hex	78	0.091	0.041	3.1	2.26	80	0.06	0.133	5.25	5.05
Gly	52	0.038	0.055	1.44	1.13	60	0.015	0.159	3.06	2.01
PBOX	λ_{irr}=365 nm					λ_{irr}=405 nm				
EtOH	69	1.03	0.155	4.1	3.1	74	0.71	0.41	4.3	4.1
ACN	77	1.13	0.101	5.1	4.2	81	0.79	0.39	5.2	5
Hex	72	0.243	0.091	3.0	2.8	79	0.62	0. 31	3.1	2.8
Gly	53	0.154	0.165	1.4	1.3	54	0.44	0.48	1.6	1.5
PyBOX	λ_{irr}=365 nm					λ_{irr}=405 nm				
EtOH	69	0.09	0.045	4	3.1	70	0.046	0.025	4.3	3.9
ACN	73	0.099	0.043	4.9	3.9	71	0.059	0.024	4.7	3.5
Hex	71	0.0835	0.048	2.8	2.4	72	0.018	0.021	3.1	2.9
Gly	51	0.03	0.032	1.1	0.989	52	0.025	0.028	1.2	0.9

described, as a representative example, Fig. 4. A 3 ml ethanolic solution (ca. 2×10^{-5} M) of an isomerically pure trans dyes was irradiated in a quartz cuvette at 25 °C. Upon irradiation of the trans solution, the absorption spectra were recorded as a function of irradiation time until the PSS was reached. As the irradiation time proceeds, the absorbance of the long-wavelength band (λ_{max}=320, 344, 346 and 386 nm for StBOX, NBOX, PBOX and PyBOX, respectively) decreases with the appearance of isosbestic points at (269 nm), (260,305 nm), (292 nm), (288, 353 nm), respectively. At the same time the absorbance of the short-wavelength bands (λ_{max}=248, 281, 286 and 302 nm, respectively) show concomitant increase. These changes were attributed to the photochemical trans-cis isomerization. The isomerization can also occur through a rotation mechanism [57], which involves a $\pi\rightarrow\pi^*$ transition ($S_0\rightarrow S_2$). As shown, replacement of phenyl ring in StBOX by large polycyclic moieties, naphthyl, phenanthryl or pyrenyl affects the time needed for reaching the PPS. For example, the cis form of StBOX, NBOX, PBOX and PyBOX in Hex takes 270, 180, 160 and 95 min, respectively, to reach the PPS. At the same time the intensities of the fluorescence spectra decrease reaching photostationary states without appearance of new bands (Fig. 5) this indicates that the photoproducts are non-fluorescent. The trans-cis interconversion during irradiation was also evidenced by the appearance of clear isosbestic points in the UV Vis-spectra.

In order to confirm the achievement of the PSS, the plots of the absorbance changes at absorption maxima vs. the irradiation time (t) at λ_{irr}=365 nm, in Gly have been examined (Insets of Fig. 5). As can be seen, the absorbance of the investigated dyes and their absorption maximum decreases gradually until reaching to a steady value, which characterized the photostationary state.

A cursory glance on data reported in Table 3, it was found that the $\phi_{t\rightarrow c}$ increases slightly as the solvent polarity increases following the order ACN>EtOH>Hex, excluding Gly. This behavior has been ascribed to a decrease in activation energy of the $1_{t^*}\rightarrow1_{p^*}$ twisting process, where the polar solvent stabilizes the 1_{p^*} configuration more than 1_{t^*}. Furthermore, in Gly, the value of $\phi_{c\rightarrow t}$ is larger than $\phi_{t\rightarrow c}$ in all cases. This behavior could be explained by solvent viscosity effects, where in this case, the trans-isomer encounters the substantial restrictions through increasing the viscosity of the medium which decreases the free volume necessary for rotational motions, thus reducing its tendency to isomerize into the cis form.

The percentage of the cis isomers (%cis) at the photostationary state have been calculated in different solvents by using Fischer's Method [58] and the obtained data

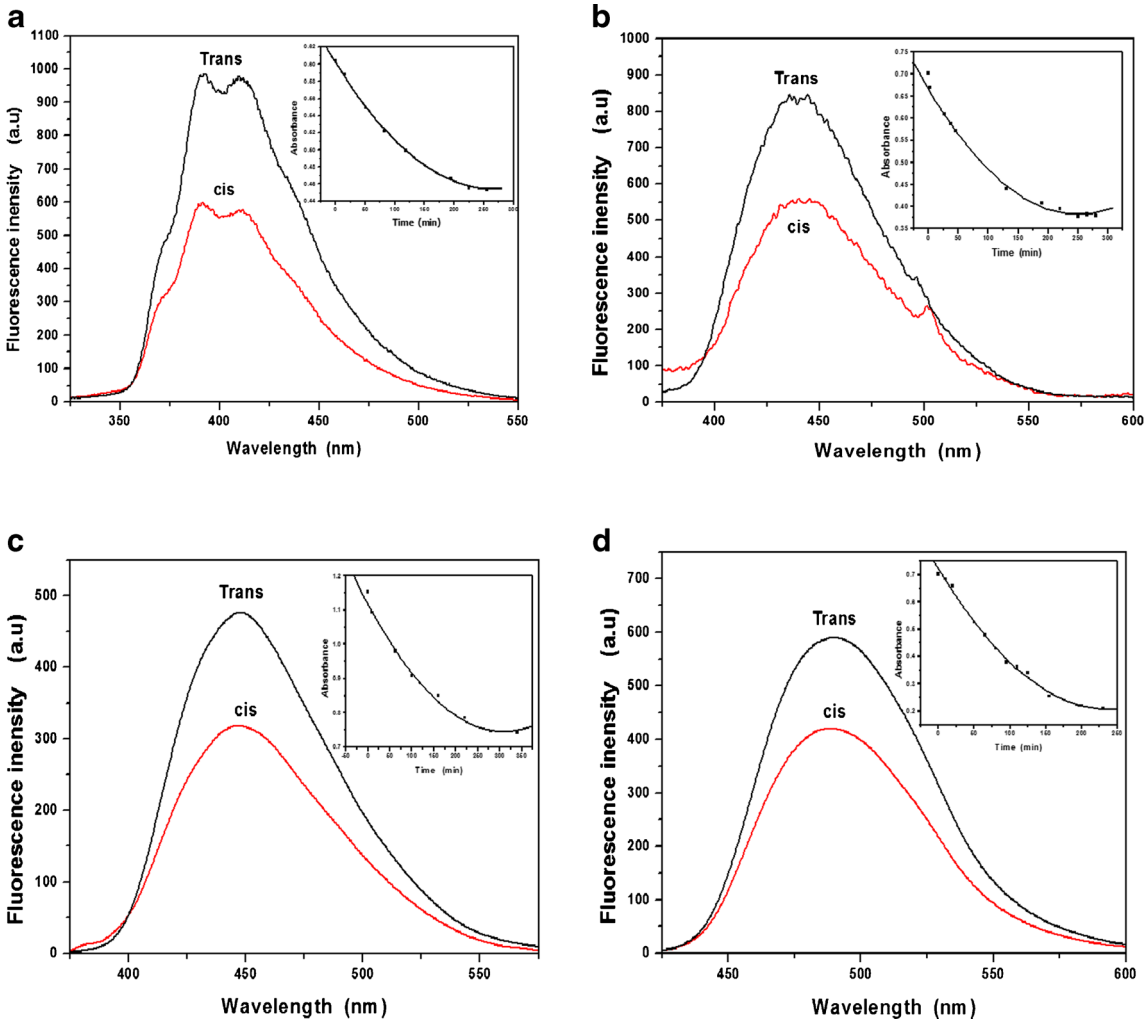

Fig. 5 Fluorescence spectra recording during irradiation of **a** StBOX, **b** NBOX, **c** PBOX, and **d** PyBOX in Gly (at 405 nm)

were summarized in Table 3. It was found that the composition of the photostationary state is displaced to the cis-isomer rich-side (contains from 51 to 85 % cis, depending on the ring size and the nature of the used solvent). In all cases, %cis enhances, to some extent, with decreasing the solvent polarity and decreases clearly with increasing solvent viscosity. For example, changing the solvent from EtOH to Hex causes an increase of the %cis at the PSS of StBOX, NBOX, PBOX and PyBOX from 70, 76, 74 and 70 to 79, 80, 78 and 72 %, respectively upon irradiation at 405 nm. However, its %cis drops to 58, 60, 54 and 52 % in Gly which is highly viscous solvent, for StBOX, NBOX, PBOX and PyBOX, respectively. It is concluded from this result that there are two operating parameters of the solvent (polarity and viscosity) that control the concerned decay process. However, the role of viscosity of the solvent increase as the ring size of aryl moiety becomes larger. On the other hand, the ring size has obvious effect on the photostationary state composition. Replacement of phenyl ring with large polycyclic moieties, naphthyl, phenanthryl and pyrenyl ones decrease % cis at the same photostationary state. As a representative example, the %cis at the same photostationary state decreases from 85 % for StBOX to 84, 81 % to 71 % for NBOX, PBOX and PyBOX in ACN upon irradiation at 405 nm, respectively. This could be attributed to the role of steric hindrance of the aryl moiety and the twisting between the hydrogen atoms of ethylenic bridge with the aryl rings in these polycyclic derivatives. Also, it is necessary to calculate the partial rate constants of the photoisomerization for the investigated dyes, because the rate at which olefinic compounds undergo isomerization is of practical importance since application of functional materials requires both structural homogeneity and stability. In all cases, the partial rate constants for trans→cis and cis→trans reactions have the same trend as the partial quantum yields where $k_{t\rightarrow c}$ values are higher than those of $k_{c\rightarrow t,}$ as shown in Table 3. All the obtained results suggested that, these dyes can serve as candidates for data storage applications which proclaim the applicability of these dyes in the industrial field.

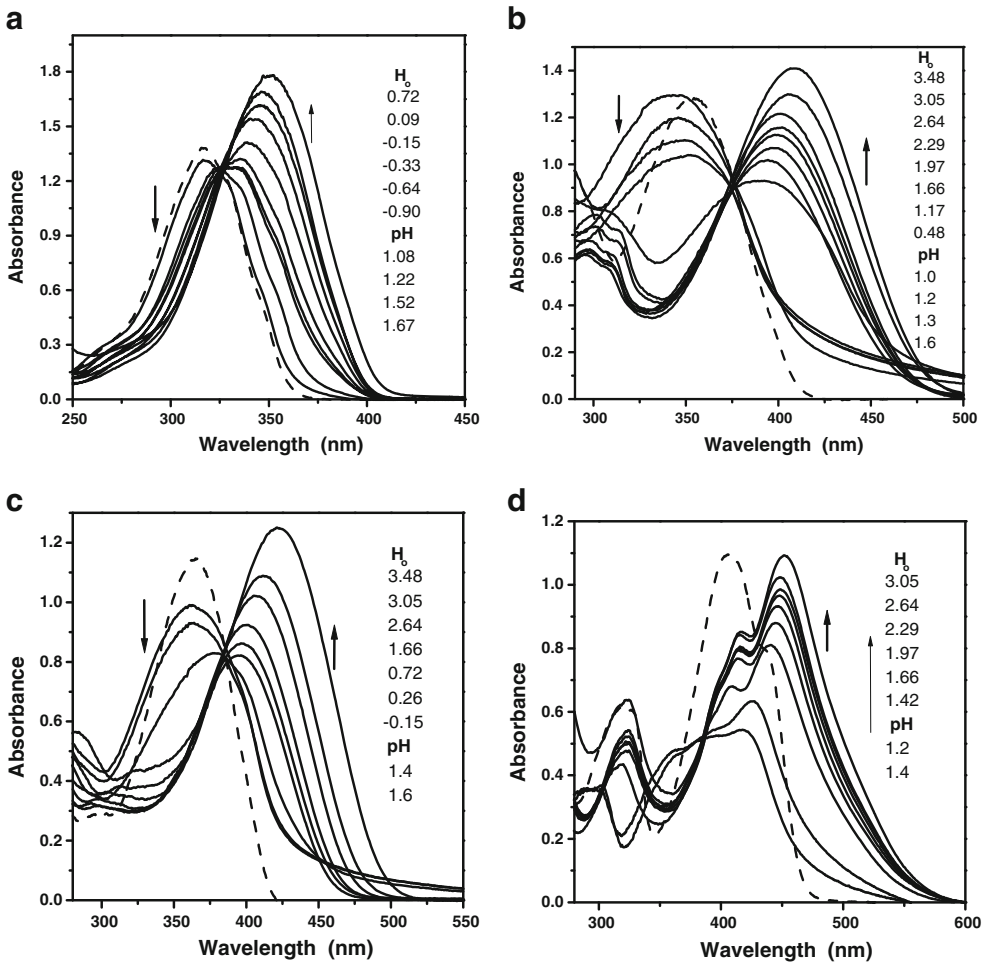

Fig. 6 Absorption spectra of **a** StBOX, **b** NBOX, **c** PBOX and **d** PyBOX at different pH/H_o values. The dashed line shows the absorption spectra of the neutral form

Acidochromic Behavior of the Investigated Diarylethylenes

In order to sense and characterize the effect of H^+ ions on the spectral behavior of the investigated dyes, their electronic absorption and emission spectra were measured at different pH/H_o values. Firstly, the absorption and emission spectra of the investigated dyes have been studied in universal buffer solutions of varying pH values (pH=1.2–12). It was found that, the shape of both absorption and emission spectra doesn't change at pH greater than 1.92, while at pH within the range 1.2–1.92, the spectra change slowly. So, in order to study the effect of acidity on the spectral behavior of the investigated dyes, the absorption and emission spectra of the investigated dyes were measured at pHs lower than 1.8 and at different hydrogen ion concentrations (H_o) using phosphoric acid. Figure 6 shows the absorption spectra of StBOX, NBOX, PBOX and PyBOX at different pH/H_o values, while the spectral data are compiled in Table 4. As can be seen, upon increasing the acid concentration (by using relatively lower pH and H_o values), the long-wavelength absorption bands are shifted to the longer wavelength, with a decrease in their intensities. The absorption maxima of StBOX, NBOX, PBOX and PyBOX were shifted from 317, 345, 363 and 434 nm (corresponding to the neutral form) to 350, 407, 422 and 454 nm, respectively, at higher H_o value. This red shifted band was due to protonation of the heterocyclic nitrogen in benzoxazole moiety with the formation of monocation which suffers stronger intramolecular charge transfer interactions compared to their neutral forms, Table 4. This conclusion is in a good agreement with theoretical calculations where the charge density on the nitrogen atom of StBOX, NBOX, PBOX and PyBOX in the

Table 4 Spectral data of both the neutral and protonated forms of the investigated diarylethylenes as well as the ground (pK) and excited (pK*) protonation constants

Dye	Neutral form		Protonated form		λ_{iso} (nm)	pK	pK*
	λ_a (nm)	λ_f (nm)	λ_a (nm)	λ_f (nm)			
StBOX	317	425	350	494	327	0.22	5.56
NBOX	345	448	407	496	375	0.27	6.67
PBOX	363	475	422	539	392	0.56	7.9
PyBOX	434	555	454	581	350, 392	2.2	5.02

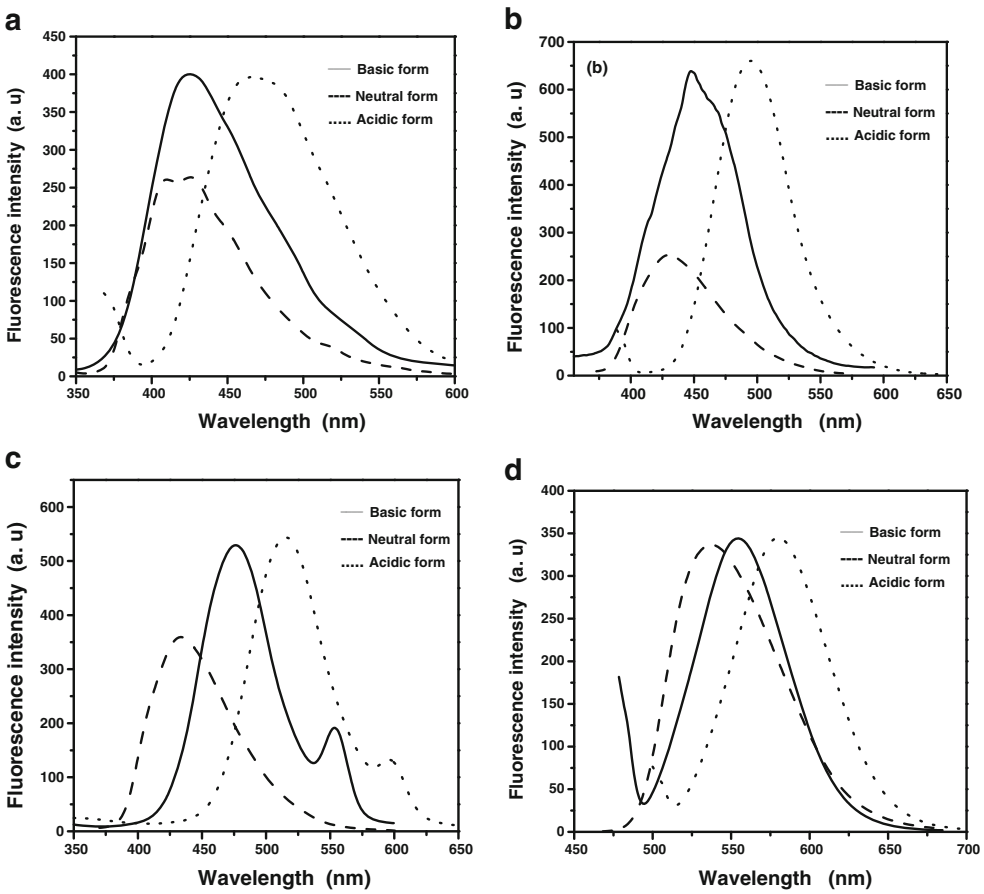

Fig. 7 Fluorescence spectra of **a** StBOX, **b** NBOX **c** PBOX, and **d** PyBOX in pH and H_o values and neutral form

excited state was -0.4706, -0.0.4834, -0.5267 and -0.4829e, while in the ground state, the charge density of the similar nitrogen atom of these dyes was -0.5132, -0.4966, -0.6301 and -0.5062e, respectively. The shifts in the absorption maxima between the two forms (depronated protonated) depend on the nature and the structure of the investigated dyes. In all cases, the gradual change of the spectra, from the neutral to highly acidic media is accompanied by the appearance of one isosbestic poins at 327, 375 and 388 nm for StBOX, NBOX and PBOX, respectively, while, PyBOX shows two isosbestic points at 355, 392 nm. This indicates the formation of acid–base equilibria and confirming the protonation of the nitrogen of benzoxazole moiety at the used pH's and H_o values. In addition, the spectral changes which associated with a bathochromic shift of the absorption maximum, is termed as halochromism [59].

Figure 7 shows the fluorescence spectra of the investigated dyes in solutions of various pH's and H_o values. The fluorescence spectra of StBOX, NBOX, PBOX and PyBOX are red shifted by 69, 48, 64 and 26 nm, respectively, on going from the neutral to acidic media, confirming the protonation of the nitrogen atom of benzoxazole moiety with the formation of the monocation. The halochromic behavior of the previously mentioned dyes denotes that these dyes can be utilized as acid–base indicators.

Finally, the ground state protonation constants (pK) were calculated from the pH/H_o dependent absorption spectra, whereas the excited state protonation constants (pK*) were calculated using Forster cycle [60]. The obtained values are listed in Table 4. It was found that pK^* values of the excited state are larger than pK values calculated for the ground state, indicating that these molecules become much stronger bases upon excitation, as found for the aza-analogues of several diarylethenes [61–65] and the corresponding dienes [66]. Also, the pK* values calculated using either the absorption or fluorescence spectral shifts are largely different from each other. This can be attributed to the difference in solvent relaxation of the conjugate acid–base pair in the ground and excited states [67].

Conclusion

The photophysical and photochemical behaviors of newly synthesized push-pull dyes were tuned by the ring size, solvent polarity and protonation using steady state absorption and emission techniques. The absorption and fluorescence studies show that the excited states of these dyes are more

polar than the ground state. The higher values of their dipole moments in the excited state than those in the ground state suggest that these dyes can serve as good candidate components of nonlinear optical materials. In addition, the trans→ cis photoisomerization quantum yields values depend on the ring size and the solvent characteristics like the polarity and viscosity. These effects on both the fluorescence and isomerization quantum yields, suggested that the two-deactivation pathways are competitive. Also, the molecular motion that occurs in the isomerization process has facilitated the development of molecular devices. Finally, the halochromic behaviors of the investigated dyes promise them to act as acid–base indicators.

References

1. Mataga N (1984) Photochemical charge transfer phenomena-picosecond laser photolysis studies. Pure Appl Chem 56:1255–68
2. Grabowski ZR, Rotkiewicz K, Siemiarczuk A, Cowley DJ, Baumann W (1979) Twisted intramolecular charge transfer states (TICT). A new class of excited states with a full charge separation. Nouv J Chim 3:443–54
3. Duan X, Konami H, Okada S, Oikawa H, Matsuda H, Nakanishi H (1996) Second-order hyperpolarizabilities of stilbazolium cations studied by semiempirical calculation. J Phys Chem 100:17780
4. Shaikh M, Mohanty J, Singh PK, Bhasikuttan AC, Rajule RN, Satam VS, Bendre SR, Kanetkar VR, Pal H (2010) J Phys Chem A 114:450
5. Cheng T, Li F, Huang C–H, Wang S, Huang W, Gong Q (2002) J Phys Chem B 106:10041
6. Koti ASR, Bhattacharjee B, Haram NS, Das R, Periasamy N, Sonawane ND, Ragnekar DW (2000) Photophysics of some styryl thiazolo quinoxaline dyes in organic media. J Photochem Photobiol A 137:115–123
7. Sertova N, Nunzi JM, Petkov I, Deligeorgiev T (1998) Photochromism of styryl cyanine dyes in solution. J Photochem Photobiol A 112:187
8. Panigrahi M, Dash S, Patel S, Behera PK, Mishra BK (2007) Reversal in solvatochromism in some novel styrylpyridinium dyes having a hydrophobic cleft. Spectrochim Acta A 68:757–762
9. Shim T, Lee MH, Kim D, Ouchi Y (2008) Comparison of photophysical properties of the hemicyanine dyes in ionic and non-ionic solvents. J Phys Chem B 112:1906–1912
10. Strehmel B, Seifert H, Rettig W (1997) Photophysical properties of fluorescence probes II: a model of multiple fluorescence for stilbazolium dyes studied by global analysis and quantum chemical calculations. J Phys Chem B 101:2232–2243
11. Kim J, Lee M (1999) Excited-state photophysics and dynamics of a hemicyanine dye in AOT reverse micelles. J Phys Chem A 103: 3378–3382
12. Gruen H, Gorner H (1989) Trans.fwdarw. cis photoisomerization, fluorescence, and relaxation phenomena of trans-4-nitro-4′-(dialkylamino)stilbenes and analogues with a nonrotatable amino group. J Phys Chem 93:7144–7152
13. Bartocci G, Mazzucato U, Massetti F, Galiazzo G (1980) Excited state reactivity of aza aromatics. 9. Fluorescence and photoisomerization of planar and hindered styrylpyridines. J Phys Chem 84:847–851
14. Foldiak G, Schuler RH (1978) Rate constants for the scavenging of radicals by iodine. J Phys Chem 82:2756–2757
15. Huang Y, Cheng T, Li F, Luo C, Huang C, Cai Z, Zeng X, Zhou J (2002) Photophysical studies on the mono- and dichromophoric hemicyanine dyes II. Solvent effects and dynamic fluorescence spectra study in chloroform and in LB films. J Phys Chem B 106:10031–10040
16. Pham THN, Clarke RJ (2008) Solvent dependence of the photochemistry of styrylpyridinum dye RH421. J Phys Chem B 112:6513–6520
17. Huang Y, Cheng T, Li F, Huang C, Hou T, Yu A, Zhao X, Xu X (2002) Photophysical studies on the mono- and dichromophoric hemicyanine dyes I. Photoelectric conversion from the dye modified ITO electrodes. J Phys Chem B 106:10020–10030
18. Messier J, Kajzar F, Prasad P (Eds.) (1991) Organic molecules for nonlinear optics and photonics, Klumer Academic Publishers
19. Kato S, Diederich F (2010) Non-planar push–pull chromophores. Chem Commun 46:1994–2006
20. Yin M, Li HP, Tang SH, Ji W (2000) Appl Phys B 70:587
21. Lagadic I, Lacroix PG, Cle'ment R (1997) Layered MPS (M=Mn, Cd) thin films as host matrixes for nonlinear optical material processing. Chem Mater 9:2004–2012
22. Duan XM, Konami H, Okada S, Oikawa H, Matsuda H, Nakanishi H (1996) Second-order hyperpolarizabilities of stilbazolium cations studied by semiempirical calculation. J Phys Chem 100:17780–17785
23. Kim OK, Choi LS, Zhang HY, He XH, Shih YH (1996) J Am Chem Soc 118:12220–12221
24. Zhou G, Wang D, Ren Y, Yang S, Xu X, Shao Z, Cheng X, Zhao X, Fang Q, Jiang M (2002) Temporal and spectral properties of picoseconds two-photon pumped cavity lasing of an organic dye HEASPS. Appl Phys B 74:147–149
25. Zheng Q, He GS, Lin T-C, Prasad PN (2003) Synthesis and properties of substituted (*p*-aminostyryl)-1-(3-sulfooxypropyl)pyridinium inner salts as a new class of two-photon pumped lasing dyes. J Mater Chem 13:2499–2504
26. Zhang J, Davidson RM, Wei MD, Loew LM (1998) Membrane electric properties by combined patch clamp and fluorescence ratio imaging in single neurons. Biophys J 74:48–53
27. Perron A, Mutoh H, Launey T, Knopfel T (2009) Red shifted voltage sensitive fluorescent proteins. Chem Biol 16:1268
28. Baxter DF, Kirk M, Garcia AF, Raimondi A, Holmqvist MH, Flint KK, Bojanic D, Distefano PS, Curtis R, Xie Y (2002) A novel membrane potential-sensitive fluorescent dye improves cell-based assays for ion channels. J Biomol Screen 7:79–85
29. Kabatc J, Pietrzak M, Pączkowski J (1998) Macromolecules 31: 4651–4654
30. Wang ZS, Li FY, Huang CH, Wang L, Wei M, Jin LP, Li NQ (2000) Photoelectric conversion properties of nanocrystalline TiO2 electrodes sensitized with hemicyanine derivatives. J Phys Chem B 104:9676–9682
31. Li F-Y, Zheng J, Huang C, Jin L, Zhuang J, Guo J, Zhao X, Liu T (2000) Novel multifunctional umbrella molecule material combining photoelectric conversion and second-order optical nonlinearities in langmuir-blodgett monolayers. J Phys Chem B 104:5090
32. Riego E, Hernández D, Albericio F, Álvarez M (2005) Directly linked polyazoles: important moieties in natural products. Synthesis 2005:1907–1922
33. Hughes RA, Moody CJ (2007) From amino acids to heteroaromatics-thiopeptide antibiotics, nature's heterocyclic peptides. Angew Chem Int Ed 46:7930–54
34. Whitesides GM, Matthias JP, Seto CT (1991) Molecular self assembly and nanochemistry: a chemical strategy for the synthesis of nanostructures. Science 54:1312
35. Lehn JM (2002) Toward self-organization and complex matter. Science 295:2400–2403
36. Ikkala O, ten Brinke G (2002) Functional materials based on self-assembly of polymeric supramolecules. Science 295:2407–2409

37. Kolev T, Koleva BB, Stoyanov S, Spiteller M, Petkov I (2008) The aggregation of the merocyanine dyes depending of the type of the counterions. Spectrochim Acta A 70:1087–96
38. Abd El-Aal RM, Shindy HA, Koraiem AIM (1997) Synthesis & electronic absorption spectra of some new penta & dimethine cyanine dyes. Heteroat Chem 8:259–266
39. Koraiem AIM, Shindy HA (1998) Orientation in the synthesis & absorption spectra of 1H-pyrazolo(4,3-d) 1,3-oxazole methine cyanine dyes. Chem Pap 52:762–770
40. Koraiem AIM, El-Maghraby MA, Khalafalla AK, Shindy HA (1989) Studies on the synthesis & solvatochromic behaviour of mono & trimethine cyanines. Dyes Pigments 11:47–63
41. Masaund MS, Khalil EA, El-Sayed El Shereafy E, El-Enein SA (1990) Thermal and electrical behaviour of nickel (II) and copper (II) complexes of 4-acetamidophenylazo-p-cresol (4-acetylamino-2-hydroxy-5-methyl azobenzene). J Therm Anal 36:1033
42. Egli R (1991) Color Chemistry The Desing and Synthesis of Organic Dyes and Pigments, ed. A.T. Peters, H.S. Freeman, Elsevier, London
43. Feringa BL, Delden RA, Wiel MKJ (2001) Molecular Switches; Feringa B. L, Ed.; Wiley-VCH: Weinheim, Germany, p 123
44. Fan MG, Yu L, Zhao W (1999) Organic Photochromic and Thermochromic Compounds, Vol 1, Crano JC, Guglielmetti RJ, Eds.; Plenum Press: New York, p 141
45. Kobatake S, Yamashita I (2008) A two-tap Schlenk adapter connected to a bubbler and an argon/vacuum manifold. Tetrahedron 85:64–71
46. Vernigor EM, Shalaev VK, Novosel'tesva LP, Luk'yanets EA, Ustenko AA, Zvolinskii VP, Zakharov VF (1980) Khim Geterotsikl Soedin 5:604
47. Rochester CH (1970) Acidity functions. In: Organic chemistry, a series of monographs, vol. 17. New York, NY, Academic Press
48. John VM, Mary AM, Huber JR (1976) Fluorescence quantum yield determinations. 9,10-Diphenylanthracene as a reference standard in different solvents. J Phys Chem 80:969–974
49. Gauglitz G (1981) Azobenzene as a convenient actinometer: evaluation values for UV mercury lines and for the N_2 laser line. J Photochem 15:255–257
50. Thompson MA, Glendening ED, Feller D (1994) The nature of K^+ crown-ether interactions-a hybrid quantum mechanical –molecular mechanical study. J Phys Chem 98:10465–10476
51. Tatikolov AS, Costa SMB (2007) Medium effects on the isomerization of an anionic polymethine dye. Chem Phys Lett 440:73–78
52. Kamlet MJ, Abboud J-LM, Abraham MH, Taft RW (1983) Linear solvation energy relationships: a comprehensive collection of the solvatochromic parameters, π^*, α and β, and some methods for simplifying the generalized solvatochromic equation. J Org Chem 48:2877–2887
53. Bakhshiev NG (1964) Universal intermolecular interactions and their effect on the position of the electronic spectra of molecu les in two component solutions. Opt Spectrosk 16:821–823
54. Chamma A, Viallet P (1970) Determination of the dipole moment in a molecule in an excited singlet state. C R Acad Sci Paris Ser C 270: 1901–1904
55. Hermant RM, Bakker NAC, Scherer T, Krijinen B, Verboeven JW (1990) Systematic study of a series of highly fluorescent rod-shaped donor-acceptor systems. J Am Chem Soc 112:1214–1221
56. Mazzucato U, Aloisi GG, Elisei F (1993) Cis-trans photoisomerization of 1,2-diarylethylenes; effect of charge transfer interactions. Chem Sci 105:475–486
57. Shin DM, Whitten DG (1988) Solvent-induced mechanism change in charge-transfer molecules. Inversion versus rotation paths for the Z.fwdarw. E isomerization of donor-acceptor substituted azobenzenes. J Am Chem Soc 110:5206–5208
58. Fischer E (1967) The calculation of photostionary states in systems A-B when only A is known. J Phys Chem 77:3704–3706
59. El-Daly SA, Fayed TA (1999) Photophysical properties and laser activity of 1,4-bis[β-(4-quinolyl)-vinyl]benzene. Spectrochim 55A: 2579–2591
60. Schulman SG (1971) Rev Anal Chem 11:85
61. Cauzzo G, Galiazzo G, Mazzucato U, Mongiat N (1966) Acid–base equilibria of isomeric styrylpyridines and some of their derivatives : spectrophotometric study. Tetrahedron 22:589–593
62. Bartocci G, Bortolus P, Mazzucato U (1973) Excited reactivity of aza aromatics. II. Solvent protonation effects on photoisomerization and luminescence of styrylpyridines. J Phys Chem 77:605–610
63. Favaro G, Masetti F, Mazzucato U, Bortolus P (1975) Excited state reactivity of aza aromatics. IV. Fluorescence properties and acid–base equilibria of naphthylpyridylethylenes. J Phys Chem 79:2785–2788
64. Spalletti A, Mazzucato U, Aloisi GG, Pannacci DZ (1983) Phys Chem NF 138:199
65. Gorner H, Elisei F, Mazzucato U (1991) Laser flash photolysis of trans-1,2-bis(4-pyridyl)ethylene in aqueous solution. J Phys Chem 95:4000–4005
66. Mazzucato U, Spalletti A (2003) Protonation effect on the excited state behaviour of EE-1-(n-pyridyl)-4-phenylbutadienes (n =2, 3 and 4). Photochem Photobiol Sci 2:282–288
67. Al-Ansari IAZ (1997) Ground- and excited-state properties of some 3,4-dihydro-1-(2-*p*-substituted benzylidene)naphthalenones: substituent and environmental effects. J Phys Org Chem 10:687–696